Reactor engineering models of complex electrochemical reaction schemes IV. Galvanostatic operation of series reactions with solvent decomposition

KEITH SCOTT

Department of Chemical Engineering, Teesside Polytechnic, Middlesbrough, Cleveland, TS1 3BA, UK

A mathematical analysis of series electrochemical reactions with solvent decomposition during galvanostatic batch operation is presented. Performance is compared to the equivalent system during potentiostatic operation by using the reduction of nitrotoluene to azoxytoluene as a representative model reaction scheme.

Nomenclature

C_j	bulk concentration of species j
C_{A0}	initial concentration of A
C_{Bmax}	minimum concentration of B
E	electrode potential
F	Faraday number
i_p	partial current density of Step p

i_T	total current density
k_{Lj}	mass transfer coefficient of species j
$k_f p$	electrochemical rate constant of Step p
n_p	number of electrons associated with Step p
S	electrode area
V	batch reactor volume
β	constant describing potential dependency of reaction rate constant

1. Introduction

Previous work on reactor models of complex electrochemical schemes has considered potentiostatic operation of parallel and series reactions [1], the inclusion of chemical reaction steps [2], galvanostatic operation of parallel reactions [3] and galvanostatic operation of a series reaction with electrode deactivation [4], and are all based on classical chemical and catalytic reaction engineering techniques. This paper is an extension of the galvanostatic analysis of series reactions to include the effect of solvent decomposition, e.g. hydrogen evolution. This type of system occurs frequently in electro-organic synthesis and the proposed analysis, although restrained by a number of simplifying assumptions, may prove a useful tool in data interpretation and reactor modelling. As an example, the reduction of nitrotoluene in alkaline ethanol–water electrolyte is considered.

2. Mathematical analysis

2.1. Model assumptions

Before deriving and using model equations it is always beneficial to highlight the important assumptions made, which are as follows:

    (a) all reaction steps have a pseudo first order concentration dependency

    (b) electrochemical kinetics are of the Tafel type

    (c) mass transport characteristics are represented by a mass transport coefficient k_L

    (d) solvent decomposition during electrolysis is in pure kinetic control (it is not too difficult to accommodate limiting current characteristics if appropriate)

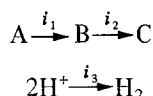   (e) the overall reaction scheme is represented by a series of rate determining steps

During galvanostatic operation the following additional assumptions are made:

859

(f) Tafel slopes for reaction Steps 1 and 2 are equal

(g) mass transport is high and not rate determining.

2.2. General reaction scheme

The reaction scheme considered is

$$A \xrightarrow{i_1} B \xrightarrow{i_2} C$$

$$2H^+ \xrightarrow{i_3} H_2$$

with reaction currents written as [1]:

$$\frac{i_1}{n_1 F} = \frac{C_A}{Y1} \tag{1}$$

$$\frac{i_2}{n_2 F} = \frac{C_A}{Y1 Y2 k_{LB}} + \frac{C_B}{Y2} \tag{2}$$

$$i_3 = n_3 F k_f 3 \tag{3}$$

where $Y1 = (1/k_f 1) + (1/k_{LA})$ and $Y2 = (1/k_f 2) + (1/k_{LB})$, with C_A and C_B being the bulk concentrations, $k_f 1$, $k_f 2$ and $k_f 3$ the electrochemical rate constants for each reaction step and k_{LA} and k_{LB} the mass transfer coefficients.

For electrolysis in a batch reactor of electrode area S and volume V design equations can be written as:

$$\frac{dC_A}{dt} = -\frac{S}{V} \frac{i_1}{n_1 F} \tag{4}$$

$$\frac{dC_B}{dt} = -\frac{S}{V} \left(\frac{i_1}{n_1 F} - \frac{i_2}{n_2 F} \right) \tag{5}$$

2.3. Potentiostatic operation

During potentiostatic batch operation the electrochemical rate constants are independent of time and the following concentration time equations can be derived:

$$\frac{C_A}{C_{A0}} = \exp\left(-\frac{St}{VY1} \right) \tag{6}$$

$$\frac{C_B}{C_{A0}} = \frac{Y2 - (1/k_{LB})}{Y1 - Y2} \left[\exp\left(-\frac{St}{VY1} \right) \right.$$

$$\left. - \exp\left(-\frac{St}{VY2} \right) \right] \quad (Y1 \neq Y2) \tag{7}$$

assuming C_B is initially zero the overall material balance is

$$C_{A0} = C_A + C_B + C_C \tag{8}$$

In reaction schemes of the series irreversible type a maximum concentration of intermediate B, C_{Bmax} is produced after a reaction time given by

$$t_{max} = \left[1 \middle/ \frac{S}{V}\left(\frac{1}{Y1} - \frac{1}{Y2} \right) \right] \ln\left(\frac{Y2}{Y1} \right) \tag{9}$$

The maximum concentration is

$$\frac{C_{Bmax}}{C_{A0}} = \frac{1}{k_f 2 Y2} \left(\frac{Y2}{Y1} \right)^{(Y1/Y1 - Y2)} \tag{10}$$

Clearly the influence of mass transport is important in determining maximum concentrations of the intermediate.

In addition the following time independent relations between C_A and C_B can be obtained when $Y1 \neq Y2$:

$$\frac{C_B}{C_{A0}} = \frac{(1/k_f 2)}{(Y2 - Y1)} \left[\left(\frac{C_A}{C_{A0}} \right)^{Y1/Y2} - \frac{C_A}{C_{A0}} \right] \tag{11}$$

and for $Y1 = Y2$

$$\frac{C_B}{C_{A0}} = \left(\frac{1}{Y1 k_{LB}} - 1 \right) \frac{C_A}{C_{A0}} \ln\left(\frac{C_A}{C_{A0}} \right) \tag{12}$$

2.4. Galvanostatic operation

During galvanostatic operation the total current density i_T is given by

$$i_T = n_1 F k_f 1 C_A + n_2 F k_f 2 C_B + n_3 F k_f 3 \tag{13}$$

With the assumption of equal Tafel slopes for Steps 1 and 2, i.e. $\beta_1 = \beta_2 = \beta$, Equation 13 can be differentiated and combined with Equations 4 and 5 (suitably modified by assuming $1/k_L = 0$) to give:

$$\left[\frac{\beta i_T}{k_f 1} + n_3 F(\beta_3 - \beta) \frac{k_f 3}{k_f 1} \right] dE = -F \left[n_1 - \frac{n_2 k_2}{k_1} \right.$$

$$\left. + n_2 \left(\frac{k_2}{k_1} \right)^2 \frac{C_B}{C_A} \right] dC_A \tag{14}$$

The time independent relations between C_A and C_B described by Equations 11 and 12 apply here when mass transport is not limiting and $\beta_1 = \beta_2$ [4] (the analysis can be developed to consider

limiting current characteristics of one or both steps in the reaction sequence: see Appendix).

Combining these equations with Equation 14 and integrating gives:

for $k_1 = k_2$

$$\left[n_3 \frac{k_f 3}{k_f 1} - \frac{i_T}{F k_f 1} \right]_E^{E_0} = n_1 (C_A - C_{A0})$$

$$- n_2 C_A \log \left(\frac{C_A}{C_{A0}} \right) \qquad (\beta_3 \neq \beta) \qquad (15)$$

where E_0 is the value of E at $t = 0$

for $k_1 \neq k_2$

$$\left[n_3 \frac{k_f 3}{k_f 1} - \frac{i_T}{F k_f 1} \right]_E^{E_0} = - \frac{C_A}{1 - (k_2/k_1)}$$

$$\times \left[\left(1 - \frac{C_A}{C_{A0}} \right) \left(n_1 - 2 n_2 \frac{k_2}{k_1} \right) \right.$$

$$\left. + n_2 \frac{k_2}{k_1} \left(1 - \frac{C_A}{C_{A0}} \right)^{k_2/k_1} \right] \qquad \beta_3 \neq \beta \quad (16)$$

Equations 15 and 16 now describe the potential variation as a function of reactant concentration.

For the condition of $\beta_3 = \beta$ the first term on the left hand side of Equations 15 and 16 drops out. By combining Equation 15 or 16 with the batch reactor design Equation 4 the concentration–time characteristics can be established.

First consider the case $\beta_3 = \beta$. With $k_1 = k_2$ we obtain:

$$- \frac{dC_A}{dt} = \frac{S}{V} \left\{ C_A \left/ \frac{1}{k_f 1_0} + \frac{F}{i_T} \left[n_1 (C_A - C_{A0}) \right. \right. \right.$$

$$\left. \left. \left. - n_2 C_A \log \left(\frac{C_A}{C_{A0}} \right) \right] \right\} \right. \qquad (17)$$

where $k_f 1_0$ is the value of $k_f 1$ at $t = 0$. On integration Equation 17 gives:

$$\frac{F}{i_T} (n_1 + n_2)(C_A - C_{A0})$$

$$+ \left(\frac{1}{k_f 1_0} - \frac{F(n_1 C_{A0} + n_2 C_A)}{i_T} \right)$$

$$\times \log \left(\frac{C_A}{C_{A0}} \right) = - \frac{S}{V} t \qquad (18)$$

With $k_1 \neq k_2$ we obtain

$$\frac{1}{k_f 1_0} \log \left(\frac{C_A}{C_{A0}} \right) - \frac{F C_{A0}}{i_T [1 - (k_2/k_1)]} \left\{ \log \left(\frac{C_A}{C_{A0}} \right) \right.$$

$$- \left(\frac{C_A}{C_{A0}} \right) + \left(n_1 - 2 n_2 \frac{k_2}{k_1} \right) + \frac{n_2 k_2}{k_1} \left[\log \left(\frac{C_A}{C_{A0}} \right) \right.$$

$$\left. \left. - \frac{k_1}{k_2} \left(\frac{C_A}{C_{A0}} \right)^{k_2/k_1} + \frac{k_1}{k_2} \right] \right\} = - \frac{S}{V} t \qquad (19)$$

Hence we can compute reaction times to reach specified conversion levels of A and then evaluate the concentration of intermediate B. Overall current efficiency $(CE)_0$ can then be obtained from

$$(CE)_0 = \frac{n_1 F C_B V}{S i_T t} \qquad (20)$$

The cases when $\beta_3 \neq \beta$ will in general (excepting perhaps when $\beta_3/\beta = 2$ or 0.5) require numerical integration of the expression

$$\int_{C_{A0}}^{C_A} \frac{dC_A}{C_A f(C_A)} = - \frac{S}{V} t \qquad (21)$$

where $f(C_A)$ is the expression for $k_f 1$ in Equations 15 and 16. This may readily be accomplished using standard library programmes. A quick concentration–time history may also be established from simple graphical integration.

These model equations will now be applied to the electrochemical reduction of nitrotoluene to azoxytoluene in alkaline ethanol water electrolyte.

3. Results and discussion

The electroreduction of nitrotoluene to azoxytoluene according to Janssen and Barendrecht [5, 6] is as follows.

Nitrotoluene undergoes a two-electron transfer to nitrosotoluene

$$C_7 H_7 NO_2 \xrightarrow[- H_2 O]{+ 2e + 2 H^+} C_7 H_7 NO$$

nitrotoluene   nitrosotoluene
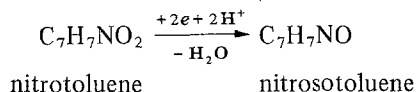
Nitrosotoluene then undergoes a fast single-electron reduction to the radical anion, which dimerizes to produce azoxytoluene.

$$C_7 H_7 NO \xrightarrow{+ e} C_7 H_7 NO^-$$

nitrosotoluene

$$2 C_7 H_7 NO^- \xrightarrow[- H_2 O]{+ 2 H^+} C_{14} H_{14} N_2 O$$
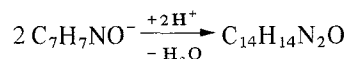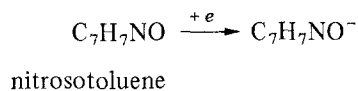
Azoxytoluene is then further reduced to form hydrazotoluene

$$C_{14}H_{14}N_2O \xrightarrow[-H_2O]{+4e+4H^+} C_{14}H_{16}N_2$$

azoxytoluene   hydrazotoluene
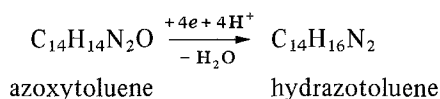
If the second and third steps of the reaction sequence are assumed fast the overall scheme is the classic three component series reaction:

nitrotoluene $\xrightarrow{i_1}$ azoxytoluene $\xrightarrow{i_2}$ hydrazotoluene
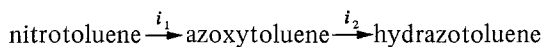
which may occur simultaneously with hydrogen evolution.

The reduction is effective on a variety of cathode materials, e.g. lead, stainless steel and platinum, and operates well at temperatures of 50–60° C.

The published experimental work of Janssen and Barendrecht [5, 6] will be used in this analysis. Their kinetic measurements [6] show well-defined limiting current regions and, hence, mass transport is important, especially if low concentrations are used. Their production data [5] is in general accord with the simplified reaction mechanism but some nitrosotoluene is produced at low nitrotoluene concentrations.

3.1. Data analysis: potentiostatic operation

Fig. 1 shows experimental data (from Janssen and Barendrecht [5]) for nitrotoluene reduction in the form of azoxytoluene production vs nitrotoluene
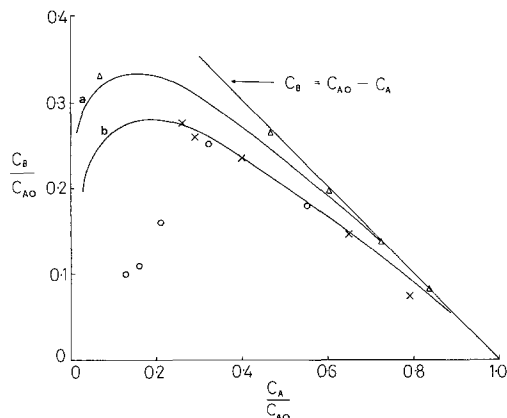

Fig. 1. Experimental data plot of azoxytoluene concentration vs nitrotoluene concentration. $\triangle$ – Pt cathode, $-1150\,\text{mV}$, $C_{A0} = 0.5\,\text{M}$; $\circ$ – Pb cathode, $-1050\,\text{mV}$, $C_{A0} = 0.095\,\text{M}$; $\times$ – Pt cathode, $-1150\,\text{mV}$, $C_{A0} = 0.028\,\text{M}$. Theoretical plots (a) $k_1/k_L = 5$, $1/k_2 = 0$; (b) $k_1/k_2 = 5$, $k_f 1/k_L = 0.5$.

concentration for two cathodes and three initial concentrations. The data show the general series reaction behaviour, i.e. azoxytoluene going through a maximum. However, at high conversions and low initial concentrations on lead, the azoxytoluene concentration falls rapidly due to additional by-product formation. To adequately correlate these data we need reliable mass transport characteristics for the experimental system and kinetic measurements which are not available. However, order of magnitude estimations of parameters can be used to fit the data. This serves the purpose at hand, i.e. the prediction of typical series reaction characteristics during galvanostatic operation and not an accurate simulation of azoxytoluene production.

Plotted on Fig. 1 are two predicted performance characteristics using a ratio of $k_1/k_2 = 5$. One curve is without mass transport limitations, (a), and the other includes mass transport limitations, (b), (using a ratio of $k_f 1/k_L = 0.5$). From this it is clear that operation with mass transport limitations causes a reduction in the amount of intermediate product. At low initial concentrations, the experimental data agree well with Curve b whereas at the higher initial concentration the data tend to fit Curve a. This disagreement may well be due to an imbalance in reported experimental material, unidentified products or an inadequate model.

3.2. Galvanostatic operation

Typical concentration–time characteristics for nitrotoluene (A) and azoxytoluene (B) are presented in Fig. 2 based on the simple series reaction with hydrogen evolution model. The current density is $1000\,\text{A m}^{-2}$, $C_{A0} = 0.5\,\text{M}$, $k_f 1_0 = 3 \times 10^{-6}$ and $k_1/k_2 = 5$, and transport limitations are ignored. The maximum production of B at low conversions is apparent (note that 2 mol A $\rightarrow$ 1 mol B). The effect of the hydrogen reduction reaction is to reduce the rate of conversion of A (cf. curve with no hydrogen evolution) and the production of B at the expense of the overall current efficiency for the reaction*.

* The concentration of C_B during galvanostatic operation is calculated from the expression [4]:

$$\frac{C_B}{C_{A0}} + \left(1 + \frac{n_1}{n_2}\right)\left(\frac{C_A - C_{A0}}{C_{A0}}\right) = -\frac{i_T S}{n_2 F C_{A0} V} \quad (F1)$$
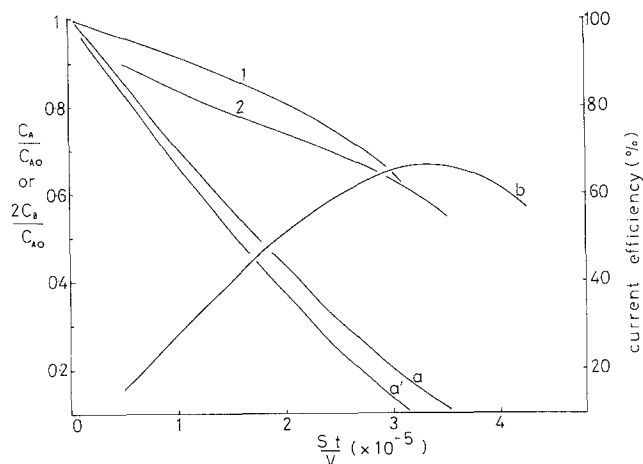
Fig. 2. Typical theoretical concentration–time characteristics for the reduction of nitrotoluene to azoxytoluene (1000 A m^{-2}, $C_{A0} = 0.5$ M, $k_f 1_0 = 3 \times 10^{-6}$, $k_1/k_2 = 5$). (a) nitrotoluene; (a') nitrotoluene without hydrogen evolution; (b) azoxytoluene; 1 current efficiency with no hydrogen evolution; 2 current efficiency with hydrogen evolution.

A plot of overall current efficiency vs time is also given in Fig. 2 and can be compared to the case with zero hydrogen reduction. The similarity between the two current efficiencies at large reaction times is attributable to the fact that without hydrogen evolution the reduction of B to C (and hence inefficiency) occurs earlier.

Fig. 3 compares the performance of the system during galvanostatic operation and potentiostatic operation where it is clear that, although maximum values of C_B are equivalent, the performance depends significantly on reaction time.

4. Conclusions

It has been shown that within a simple modelling framework of a series reaction the onset of solvent decomposition can be accommodated during the prediction of concentration–time characteristics for galvanostatic operation. The inclusion of mass transport limitations during galvanostatic operation may be important for certain systems as its effect is likely to be similar to that demonstrated during potentiostatic operation. Work is presently under way on this topic [7]. A mathematical model for azoxytoluene production may possibly be developed from this basic analysis.

Appendix

The behaviour of series reactions during galvanostatic operation where one or more of the steps is at its limiting current can be developed as given below.

A.1. *First step at limiting current: no solvent decomposition*

The reaction current density i_1 in this case is:
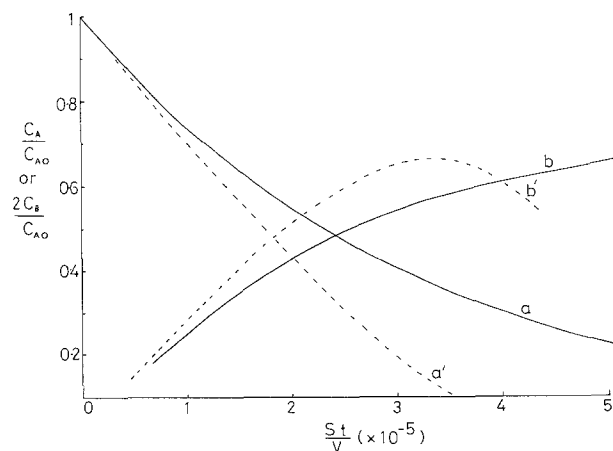
$$i_1 = n_1 F k_{LA} C_A \qquad (A1)$$

Fig. 3. Comparison of the production of azoxytoluene for potentiostatic operation (———) and galvanostatic operation (– – –). (a) and (a') nitrotoluene; (b) and (b') azoxytoluene.

which in a batch reactor gives the concentration variation as:

$$\frac{C_A}{C_{A0}} = \exp\left(-\frac{Sk_{LA}t}{V}\right) \qquad (A2)$$

During galvanostatic operation the current density for the second step is therefore given by:

$$i_2 = i_T - n_1 F k_{LA} C_{A0} \exp\left(-\frac{Sk_{LA}t}{V}\right) \; (A3)$$

which in a batch operation gives the concentration variation of B as:

$$\frac{C_B}{C_{A0}} = \frac{Si_T t}{V_1 n_2 F C_{A0}} + \frac{n_1}{n_2}\left[\exp\left(-\frac{k_{LA}St}{V}\right) - 1\right] \qquad (A4)$$

The production of B at a fixed current density is therefore controlled by the depletion of A and not in effect influenced by kinetics.

Equations A3 and A4 can be used to assess the potential variation and determine whether solvent decomposition is likely from:

$$Y2 = \frac{n_2 C_B}{i_2} = \frac{1}{k_{LB}} + \frac{1}{k_f 2} \qquad (A5)$$

If both reaction steps were at their respective limiting current then C_B will exhibit the classic series chemical reaction vs time behaviour. However, solvent decomposition will inevitably occur because of the requirements of constant current operation.

A.2. *First step at limiting current with solvent decomposition*

In this case the influence of solvent decomposition can be tested by combining the batch reactor Equation 5 for C_B with the total current density i_T in differential form to give:

$$-\frac{dE}{dt}(n_2\beta_2 k_f 2 + n_3\beta_3 k_f 3) = n_1 k_{LA}\frac{dC_A}{dt}$$

$$+\frac{n_2}{F}\frac{k_f 2}{V}S\left[i_1\left(\frac{1}{n_1}+\frac{1}{n_2}\right) - \frac{i_T}{n_2}\right] + \frac{n_3 Sk_f 2k_f 3}{V} \qquad (A6)$$

Both dC_A/dt and i_1 are known expressions as a function of time (Equation A2) and hence Equation A6 is of the type:

$$\frac{dE}{dt} = f(E, t) \qquad (A7)$$

requiring numerical integration to evaluate E as a function of time and hence C_B from Equation 13.

References

[1] K. Scott, *Electrochim. Acta* 30 (1985) 235.
[2] K. Scott, *ibid.* 30 (1985) 245.
[3] K. Scott, *J. Appl. Electrochem.* 15 (1985) 837.
[4] K. Scott, submitted to *Chem. Eng. Res. Design*.
[5] L. J. J. Janssen and E. Barendrecht, *Electrochim. Acta.* 26 (1981) 1831.
[6] *Idem, ibid.* 26 (1981) 699.
[7] N. Haines, I. F. McConvey and K. Scott, submitted to *Chem. Eng. Sci.*